https://doi.org/10.48048/tis.2025.8805

Threshold Condition of Energy Splitting for Some Classes of Symmetric Double Well Potential

Abdurrouf [*], Gancang Saroja and Muhammad Nurhuda

Department of Physics, Faculty of Mathematics and Natural Sciences, Brawijaya University, Indonesia

([*]Corresponding author's e-mail: abdurrouf@ub.ac.id)

Received: 6 August 2024, Revised: 28 August 2024, Accepted: 20 September 2024, Published: 15 November 2024

Abstract

The double-well potential (DWP) is a prevalent mathematical model for systems with 2 force centers, widely applied in quantum physics. Often expressed as a function with multiple parameters, the DWP can exhibit either single-well or double-well behavior depending on these parameters. Within the tunneling regime, optical properties are primarily characterized by the energy difference resulting from energy splitting (ES). Thus, formulating boundary conditions for the DWP and quantifying ES are critical but understudied areas. This research explores the threshold conditions for the existence of DWPs and ES in 2 common classes of symmetric DWPs: The extensively studied Razavy potentials and the more recently introduced Dong potentials. Utilizing quasi-exact solutions for Razavy potentials and the filter method for Dong potentials, we analyze the dependence of ES on DWP parameters. Our findings align well with existing numerical data, eigenfunction analysis and energy difference approaches. This innovative methodology allows for the examination of threshold conditions for higher ES, and provides an opportunity to control ES in DWPs by adjusting structural parameters.

Keywords: Dong potential, Double-well potential, Eigen-energy, Eigenfunction, Energy splitting, Filter method, Razavy potential, Threshold condition

Introduction

Two-center force phenomena are a fundamental class of interactions in physics and chemistry, characterized by the presence of 2 distinct centers of force exerting influence on a particle or system. This concept underlies a wide range of physical phenomena, from the behavior of electrons in diatomic molecules to the dynamics of planets in planetary systems [1-4]. A common mathematical model for 2-center force phenomena is the double-well potential (DWP) [5]. The DWP consists of 2 potential energy minima, separated by a central potential barrier. These minima can represent stable configurations of the system, and their symmetry or asymmetry depends on the specific nature of the forces involved.

Among the commonly used DWP models, the Razavy bistable (RB) potential [6], Konwent potential [7] and double sine hyperbolic-Gordon (DSHG) potential [8] stand out. The RB and DSHG potentials currently find application in theoretical investigating the electrical and optical properties of semiconductors through the analysis of structural parameters and the influence of external fields [9-11]. This theoretical research complements the experimental investigation into the electronic and optical properties of semiconductors [12,13]. The Konwent potential has also found application in studying various properties of semiconductors. This includes binding energy and absorption of donor impurities [14], non-linear optical phenomena (e.g., rectification, harmonic generation) [15,16] and the impact of hydrogenic impurities and structural parameters [17,18]. Additionally, the influence of external magnetic fields on the optical properties of spherical quantum dots has been explored using this potential [19]. Remarkably, these 3 models share a highly similar mathematical structure, differing only in a few parameters. Consequently, they are collectively referred to as the "Razavy class potential".

The other symmetric hyperbolic DWPs are the Dong class potential [20] depending on structure parameters a and k. The Dong potentials has been theoretically employed to investigate the influence of structural parameters and high-frequency intense laser fields on the linear and nonlinear optical properties of a GaAs quantum well [21]. Numerical results show that an increase in the structure parameter a (k) leads to an enhanced (reduced) amplitude of the total optical absorption coefficients and a blue (red) shift of the resonance energy spectrum. Furthermore, a recent study reveals that the energy difference in tunelling (non-tunelling) regime exhibits an exponential (linear) relationship with the k [22]. Dong's potential also inspired another hyperbolic DWP [23].

While the Razavy and Dong class potentials offer a wide range of applications, their effectiveness is predicated on their configuration as DWPs rather than single-well potentials (SWPs). Consequently, establishing the critical boundary between DWP and SWP regimes presents a significant challenge. Furthermore, optical properties are predominantly characterized within the tunneling regime by leveraging the energy difference arising from energy splitting (ES). This underscores the difficulty in identifying the critical conditions for DWPs with and without ES. To date, a number of studies have explored various parameters in both potential classes, resulting in the identification of conditions for SWP, DWP without ES and DWP with ES [6-8,20,22,24-29]. However, to the best of our knowledge, no study has explicitly formulated the critical conditions for the transition between these 3 states.

This paper investigates opportunities for establishing critical condition between SWP and DWP, as well as critical condition between DWP with and without ES in Razavy and Dong class potentials. The condition for ES occurs where the first excited energy levels is lower than the local maxima. As both first excited energy levels and local minima spends on the structure parameters, then the critical condition can be expressed in the structure parameters. Here, we use existing quasi-exactly solvable (QES) solution for RB potential, and extend them for DSHG and Konwent potentials. For Dong class potentials, we use numerical results obtained using our developed filter method [30-34]. We also investigate the critical condition for higher level of ES. To demonstrate the method's efficacy and reliability, we compared our findings with the eigenfunction and energy difference approaches [22], and the other available numerical data [27,28]. The proposed method can be utilized to confirm the existence of a DWP with a specific ES level, and moreover, to regulate the energy difference.

Analytical and numerical methods

Our initial investigation focuses on the RB potential, that depends on 3 parameters: α, ξ and m, and expressed as [6,35]:

$$V_{RB}(x)=\frac{\hbar^2\alpha^2}{2\mu}\left[\frac{1}{8}\xi^2\cosh^2(4\alpha x)-(m+1)\xi\cosh(2\alpha x)-\frac{1}{8}\xi^2\right]. \quad (1)$$

The RB potential offers several advantages, including its pioneering, simple mathematical form, availability of QES and versatility due to its 3 adjustable parameters. According to Eq. (1), the RB potential vanishes for $\xi=0$. DWP exists for all positive values of α. As the parameter α increases, the potential well becomes increasingly narrow and steep. Here, we focus on the RB potential that is most studied [6-8,22,24-29] and applied [12-19], namely the RB with $\alpha=1$. **Figure 1(A)** illustrates the behavior of the RB potential for fixed $\alpha=1$ and $\xi=4$. The figure reveals that the RB potential (i) transforms into a SWP for $(\xi/2)>(m+1)$, (ii) possesses a flat bottom for $(\xi/2)=(m+1)$ and (iii) emerges as DWP for $(\xi/2)<(m+1)$ [6]. Then, the critical condition for the existence of DWP is:

$$(\xi/2)=(m+1). \quad (2)$$

For $\xi=4$, Eq. (2) provides the critical condition for DWP at $m=1$, as shown in **Figure 1(A)**.

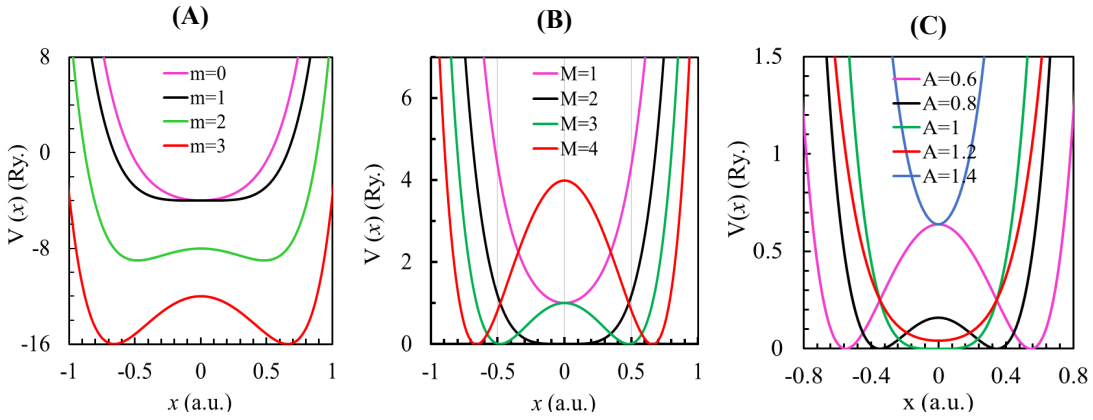

Figure 1 The profile of the RB potential (Eq. (1)) for $\alpha = 1$, $\xi = 4$ and various m (A), the DSHG potential (Eq. (4)) with $2\beta^2 = 1$, $\eta = 2$ and various M (B) and the Konwent potential (Eq. (10)) with $a = 2$, $V_0 = 4$ and various A (C).

The depth and width of this DWP increase as the absolute value of $(\xi/2)/(m+1)$ decreases. The DWP has a central local maximum $V_{\max} = -(m+1)\xi$ at $x_{\max} = 0$ and 2 symmetric local minima $V_{\min} = -\left[(m+1)^2 + \xi^2/4\right]$ located at $x_{\min} = \pm(1/2)a\cosh[2(m+1)/\xi]$. Our previous work [22] demonstrated that ES occurs (disappears) when the eigen-energy of the first excited state ε_2 is lower (greater) than the central local maximum $V_{\max}$. Consequently, the threshold condition for ES in an RB potential with $\alpha = 1$ is:

$$\varepsilon_2 + (m+1)\xi = 0 . \quad (3)$$

QES solutions for the Schrödinger equation with RB potential ($\alpha = 1$) are limited to integer values of $m = 0-7$, providing solutions for the lowest $(m+1)$ states for each m [6]. For higher m, only numerical (exact or semi-exact) solutions in terms of confluent Heun functions exist [26-29]. These QES solutions (eigenfunctions and eigen-energies) are available in explicit form for $m = 0-4$ [6,24]. For $m = 5-7$, the solution for eigen-energies requires solving a cubic equation obtained by setting the determinant of the characteristic matrix to 0 [24,25]. Using Eq. (3), we identify the critical value $\xi_{th,ES}$ that fulfills the ES threshold for any given m. Subsequently, we will derive an equation for the critical condition of ES applicable to all values m.

The second problem concerns the application of Schrödinger-like equations representing kinks and anti-kinks in thermodynamics [8,36] $\frac{1}{2\beta^2}\frac{\partial^2\psi}{\partial x^2} + [\eta\cosh(2x) - M]^2\psi = \varepsilon\psi$. This equation can be rewritten as $\frac{\partial^2\psi}{\partial x^2} + 2\beta^2[\eta\cosh(2x) - M]^2\psi = \varepsilon'\psi$. The last equation exhibits a structure similar to the Schrödinger equation in Rydberg units, with potential:

$$V_{DSHG}(x) = 2\beta^2[\eta\cosh(2x) - M]^2 . \quad (4)$$

Here, $\varepsilon' = 2\beta^2\varepsilon$. Eq. (4) has 3 real constants, which are η, M and β, where β is related to the temperature. Here, we focus on the DSHG potential that is most studied [8,36] and applied [9-11,14-19], namely the DSHG with $2\beta^2 = 1$.

The profile of the DSHG potential for $2\beta^2 = 1$ and $\eta = 2$ is depicted in **Figure 1(B)**. The potential reduces to a SWP for $\eta > M$, has a flat bottom for $\eta = M$, and exhibits a DWP for $\eta < M$ where the DPW is more pronounced for larger M [8]. Then, the critical condition for the existence of DWP in DSHG potential is:

$$\eta = M . \quad (5)$$

The DPW has a local maximum at its center $x_{\max}=0$ with $V_{\max}=(\eta-M)^2$ and 2 symmetric local minima at $x_{\min}=\pm(1/2)\cosh^{-1}(M/\eta)$ with $V_{\min}=0$. Consequently, the threshold condition for ES in DSHG potential with $2\beta^2=1$ is:

$$\varepsilon_2-(\eta-M)^2=0\,. \tag{6}$$

Using Eq. (6), we identify the critical value $\eta_{th,ES}$ that fulfills the ES threshold for any given M. Subsequently, we will derive an equation for the critical condition of ES applicable to all values M.

To obtain the eigen energies of the Schrödinger equation involving the DSHG potential, we expand Eq. (4) as $V_{DSHG,2\beta^2=1,M,\eta}(x)=\left[\frac{1}{2}\eta^2\cosh^2(4x)-2M\eta\cosh(2x)-\frac{1}{2}\eta^2\right]+(\eta^2+M^2)$. By substituting $\eta=\xi/2$ and $M=m+1$, the first term on the right-hand side of the last equation reduces to $V_{RB}(x)$ with $\alpha=1$, $m=M-1$ and $\xi=2\eta$, leading to the following relationship:

$$V_{DSHG,2\beta^2=1,M,\eta}(x)=V_{RBP,\alpha=1,m=M-1,\xi=2\eta}(x)+(\eta^2+M^2). \tag{7}$$

Eq. (7) allows us to establish a relationship between the eigen-energies of the DSHG potential and the RB potential:

$$\varepsilon_{DSHG,2\beta^2=1,M,\eta}=\varepsilon_{RB,\alpha=1,m=M-1,\xi=2\eta}+(\eta^2+M^2). \tag{8}$$

Eq. (8) enables us to obtain the QES eigen-energies with $2\beta^2=1$ for $M=1-8$, for arbitrary η. These results extend the QES which is currently available for $M=1-5$ [8, 36]. For $2\beta^{2^2}\neq 1$, we scale the results from Eq. (8) and rewrite it as:

$$\varepsilon_{DSHG,2\beta^2,M,\eta}=\frac{1}{2\beta^2}\varepsilon_{DSHG,2\beta^2=1,M'=\sqrt{2}M\beta,\eta'=\sqrt{2}\eta\beta}\,. \tag{9}$$

For $M>8$ and arbitrary η, the eigen-energy can be obtained numerically.

The third potential we investigate is the Konwent potential, expressed as [7]:

$$V_K(x)=V_0\left[A\cosh(ax)-1\right]^2. \tag{10}$$

where V_0, A and a are real constants. For $a=2$, $V_{Konwent}(x)$ simplifies as $\left[A\sqrt{V_0}\cosh(2x)-\sqrt{V_0}\right]^2$.

This simplification leads to the following relationship:

$$\varepsilon_{Konwent,a=2,V_0,A}=\varepsilon_{DSHG,2\beta^2=1,\eta=A\sqrt{V_0},M=\sqrt{V_0}}\,. \tag{11}$$

Eq. (11) allows us to establish extended QES for the Konwent potential under specific parameter conditions ($a=2$ and $\sqrt{V_0}=1-8$). which is currently only available for $\sqrt{V_0}=5$ [7]. This solution is more precise than semi-excat solution [37]. As shown in **Figure 1(C)**, the Konwent potential becomes a DWP for $A<1$, has a flat bottom for $A=1$ and reduces to a SWP for $A>1$. Then, the critical condition for the existence of DWP in Konwent potential is [7]:

$$A=1\,. \tag{12}$$

Figure 1(C) also shows that DWP has a local maximum at its center $x_{\max}=0$ with $V_{\max}=V_0(A-1)^2$. Thus the threshold condition for ES energy for Konwent potential with $a=2$ reads:

$$\varepsilon_2-V_0(A-1)^2=0\,. \tag{13}$$

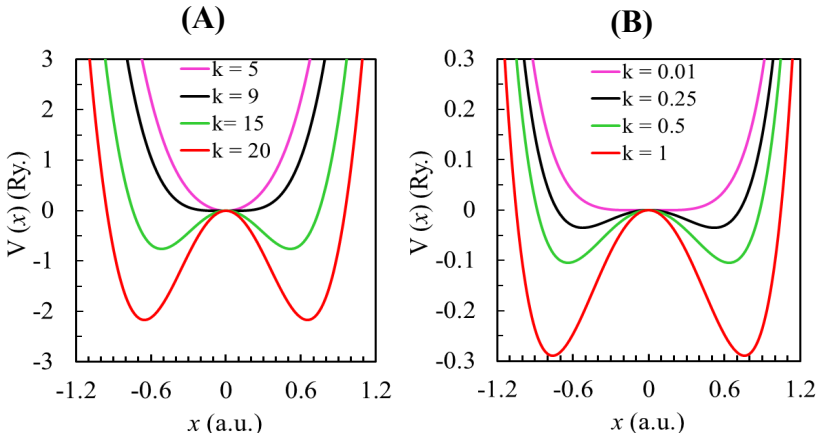

Figure 2 The profile of the first type of Dong potential (Eq. (14)) for fixed $a = 3$ with various k (A) and the second type of Dong potential (Eq. (15)) for fixed $c = 0.5$ with various k (B).

The last potential under investigation is the recently proposed symmetric hyperbolic potential, namely the Dong potential [20]. The first type of Dong potential reads:

$$V_{D1}(x) = a^2 \sinh^2(x) - k \tanh^2(x). \quad (14)$$

while the second type of Dong potential reads:

$$V_{D2}(x) = c^2 \sinh^4(x) - k \tanh^2(x). \quad (15)$$

where a, c and k are positive constants.

The potential profiles are depicted in **Figure 2(A)** for the first type and **Figure 2(B)** for the second type. Both exhibit a local maximum at its center $x_{\max} = 0$ with $V_{\max} = 0$, gives us the threshold condition for ES as:

$$\varepsilon_2 = 0. \quad (16)$$

In addition, potenttial **(14)** creates 2 symmetric local minima at $x_{\min} = \pm \operatorname{acosh}\left(\left(k/a^2\right)^{1/4}\right)$ with $V_{\min} = -\left(a - \sqrt{k}\right)^2 < 0$. Then, the double-well potential appears for $k \geq a^2$ only, reduces to a SWP for $k < a^2$ [20], and gives the critical condition for the existence of DWP as:

$$k = a^2. \quad (17)$$

However, the analytical expression for threshold condition for DWP for potential **(15)** is too complicated to write explicitly.

Results and discussion

We begin to explore the critical conditions for a DWP described by an RB potential (Eq. (1)) with $\alpha = 1$. The first critical condition ensures the formation of a DWP itself, represented by Eq. (2). The second critical condition determines when ES occurs within the formed DWP. This is achieved using Eq. (3), which likely relates the eigen-energy of the first excited states ε_2 to the RB potential parameters ξ. Here, ε_2 is obtained from the QES solution. By applying Eq. (3), we can arrive at a polynomial equation in terms of ξ. The roots of this polynomial equation then represent the $\xi_{th,ES}$ which are the threshold values that distinguish between condition with and without ES in the DWP. The $\xi_{th,ES}$ is specific for different m, as shown in **Table 1**. We note here that there is no ES for $m = 1$, regardless the value of ξ. For $m = 5-7$, $\xi_{th,ES}$ is obtained by interpolation.

Table 1 The calculated $\xi_{th,DWP}$ and $\xi_{th,ES}$ from the RB potential **(1)** with $\alpha = 1$ and $m = 1-7$. We also shows ε_2. For $m = 5-7$, ε_2 is the first eigen of characteristic matrix.

m	**Eigen energy of the first excited states,** ε_2	**[Ref.]**	$\xi_{th,DWP}$	$\xi_{th,ES}$
0	-	[6]	2	-
1	$\varepsilon_2 = \xi - 1$	[6]	4	$1/3$
2	$\varepsilon_2 = -4$	[6]	6	$4/3$
3	$\varepsilon_2 = -5 + \xi - 2\sqrt{4 + 2\xi + \xi^2}$	[6]	8	$\frac{29 + 2\sqrt{163}}{21}$
4	$\varepsilon_2 = -10 - 2\sqrt{9 + \xi^2}$	[24]	10	4
5	$\begin{vmatrix} -1+3\xi-\varepsilon & -48s & 0 \\ -2\xi & -9-\varepsilon & -5\xi \\ 0 & -\xi & -25-\varepsilon \end{vmatrix}$	[24]	12	5.491563
6	$\begin{vmatrix} 0-\varepsilon & -4\xi & 0 & 0 \\ 0 & -4-\varepsilon & -5\xi & 0 \\ 0 & -2\xi & -25-\varepsilon & -62\xi \\ 0 & 0 & -2\xi & -36-\varepsilon \end{vmatrix}$	[25]	14	7.048000
7	$\begin{vmatrix} 42\xi-1-\varepsilon & -5\xi & 0 & 0 \\ -3\xi & -9-\varepsilon & -6\xi & 0 \\ 0 & -2\xi & -25-\varepsilon & -8\xi \\ 0 & 0 & -16s & -49-\varepsilon \end{vmatrix}$	[25]	16	8.647160

Figure 3(A) presents 3 possible regime for DWP with RB potential. The black points represent $\xi = 2(m+1)$ (Eq. (2)) which is the boundary between SWP and DWP. On ther other hand, the blue points represents the boundary in the formed DWP, between DWP without and with ES. Taking the set data $(m, \xi_{th,ES})$ with $m = 1-7$, the dependence of $\xi_{th,ES}$ on m reads:

$$\xi_{th,ES} = 0.0552m^2 + 0.9607m - 0.7397. \quad (18)$$

Building on previous work, this analysis explores the splitting of higher energy levels in DWP systems [22]. This phenomenon creates sublevels within a single, originally higher-energy state, such as second splitting creates ε_3 and ε_4, and third splitting creates ε_5 and ε_6. We can further categorize DWP regime based on the highest ES. A DWP denoted as "DWP with ΔE_{ij}" signifies that the system guarantees the splitting of a higher energy level into ε_i and ε_j. This splitting is characterized by the parameter ε_j having smaller value than $V_{\max}$. **Figure 3(B)** also illustrates DWP with second-level ES ΔE_{34} characterized by $E_4 < -(m+1)\xi$ and DWP with third-level ES ΔE_{56}, characterized by $E_6 < -(m+1)\xi$. Notably, the threshold for inducing higher-level ES is observed to occur at lower values of ξ.

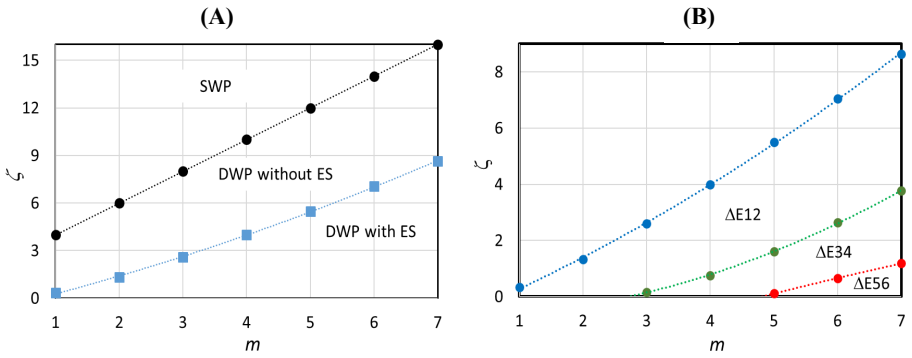

Figure 3 The 3 regimes for the RB potential **(1)** with $\alpha = 1$ and $m = 1-7$ (A), and the example of 3 regimes within DWP with ES (B).

Unfortunately, a lack of comparable numerical data, hinders our analysis. To address this, we compare our predictions using eigenfunction and energy difference approaches. In **Figure 3**, we plot the eigenfunction of the ground states ψ_1 and the first excited states ψ_2 for 3 diffrent regimes, characterized by $(m = 4, \xi = 1)$ for DWP with ES, $(m = 4, \xi = 5)$ for DWP without ES and $(m = 4, \xi = 11)$ for SWP. The eigenfunctions are shown in **Figure 4**. As expected, the 2 lowest energy eigenfunctions for $(m = 4, \xi = 1)$ appear as a symmetric and anti-symmetric pair. This indicates that both experiences tunneling, which is reflected in the splitting of their energies. This symmetric and anti-symmetric pair is absent for $(m = 4, \xi = 5)$, suggesting no splitting of energy levels. However, the ground state eigenfunction of $(m = 4, \xi = 5)$ shows a dip in its peak, which might be a hint of weak tunneling. However, the first excited state eigenfunction of $(m = 4, \xi = 5)$ shows no evidence of tunneling. In contrast, there is no evidence of tunneling in $(m = 4, \xi = 11)$ aligns with the expectations from SWP. It is also worthwhile to compare the energy difference between 2 levels, which are 0.202055 Ry for $(m = 4, \xi = 1)$, 4.150941 Ry for $(m = 4, \xi = 5)$ and 17.858215 Ry for $(m = 4, \xi = 11)$. It is observed that the energy difference in $(m = 4, \xi = 1)$ is quite small, which is typical value of energy diffeerence due to ES.

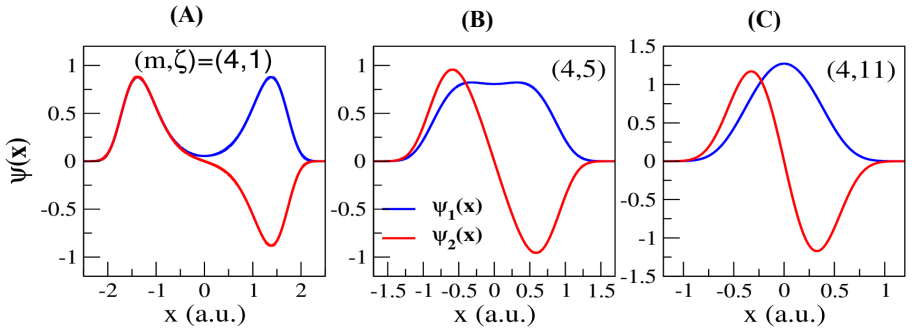

Figure 4 The ground states ψ_1 and the firs excited states ψ_2 for fixed $m = 4$ with different ξ, represents DWP with ES (A), DWP without ES (B) and SWP (C).

From the previous study [22,37-39] it was observed that the energy difference between 2 lowest energy level $\Delta E = E_2 - E_1$ is an exponential (linear) function of DWP parameter for ES (non-ES) case.

Figure 5 shows ΔE as a function of m for different value of ξ, which are $\xi = 0.1$ representing DWP with ES, $\xi = 5.5$ representing DWP without ES and $\xi = 15$ representing SWP. For $\xi = 0.1$, it is observed that ΔE is an exponential function of m, as expected. For $\xi = 5.5$ and $\xi = 15$, ΔE is a linear function of m, where the second has greater slope.

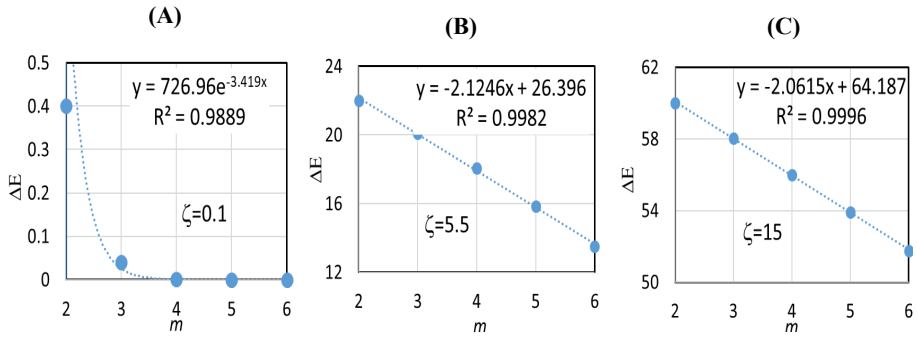

Figure 5 The energy difference between 2 lowest energy level as a function of *m*, for different ξ, represents DWP with ES (A), DWP without ES (B) and SWP (C).

Leveraging Eq. (8), we obtain the extended QES for the DSHG potential for $M = 1-8$. Using Eq. (6), the threshold condition between DWP with and without ES for DSHG potential with $2\beta^2 = 1$ reads:

$$\eta_{th,ES} = 0.0276M^2 + 0.4251M - 0.8226. \quad (19)$$

Combining with the critical condition for DWP $\eta = M$, it enables us to define boundary lines for SWP, DWP without ES and DWP with ES, as shown in **Figure 6(A)**. The figure also illustrates DWP with second-level ES ΔE_{34} characterized by $E_4 < (\eta - M)^2$ and DWP with third-level ES ΔE_{56}, characterized by $E_6 < (\eta - M)^2$. Notably, the threshold for inducing higher-level ES is observed to occur at lower values of η.

In **Figure 6(A)**, we also present other numerical data concerning the ES. The first data set is attributed to Baradaran *et al.* [27], obtained using the Bethe ansatz method (BAM). They employed parameters $2\beta^2 = 1$, $\eta = 2$ and $M = 2-12$. Their results indicate no ES for $M = 2-5$, a first-level ES of ΔE_{34} for $M = 6-8$, a second-level ES of ΔE_{34} for $M = 9-11$ and a third-level ES of ΔE_{56} for $M = 12$. The second data set is due to Sous [28], acquired through the asymptotic iteration method (AIM) with parameters $2\beta^2 = 1$, $\eta = 2$ and $M = 5-7, 8.5$. Sous [28] reported no ES for $M = 5$, first-level ES of ΔE_{34} for $M = 6-7$, and second-level ES of ΔE_{34} for $M = 8.5$. As shown in the figure, the observed phenomena align with our predictions.

Figure 6(B) directly compares our prediction with the numerical results obtained using the filter methods [30]. The figure shows 2 regimes, DWP with ES by various colors depends on the value of $\varepsilon_2 - (\eta - M)^2$. On the other hand, the regime DWP without ES, characterized by $\varepsilon_2 - (\eta - M)^2 > 0$, is shown in white. The theoretical boundary line between these regimes is plotted as a black line. We observe good agreement between the numerical and the analytical results, particularly where both predict the same boundary condition for the DWP with and without ES. These results confirm the accuracy of the filter method, demonstrating its applicability in determining eigen-energies that are not yet analytically available.

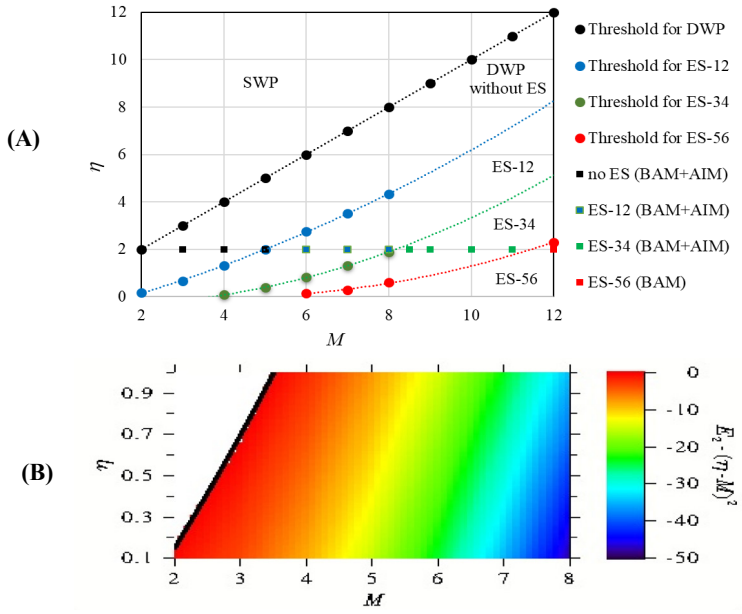

Figure 6 The 5 regimes for the DSHG potential **(3)** with with $2\beta^2=1$ and $M=2-8$ (A) and the numerical value of $\varepsilon_2-(\eta-M)^2$ (B).

Leveraging Eq. (11), we obtain the extended QES for the Konwent potential for $a=2$ and $V_0=1-64$. Using Eq. (13), the threshold condition between DWP with and without ES for Konwent potential with $a=2$ and $V_0=1-64$ reads:

$$A_{th,ES}=4x10^{-6}V_0^3-0.0006V_0^2+0.029V_0-0.0108. \quad (20)$$

Combining with the critical condition for double well potential (Eq. (12)), it enables us to define boundary lines for SWP, DWP without ES and DWP with ES for Konwent potential, as shown in **Figure 7**. The figure also displays Konwent's analytical results ($V_0=25$, $A_0=0.2$) [7] indicating a DWP with first-level ES (blue triangle). This aligns with our predictions for this regime.

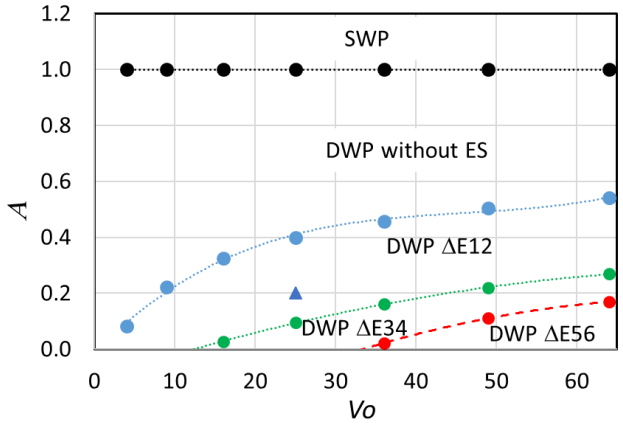

Figure 7 The 5 regimes for the Konwent potential **(10)** with with $a=2$ and $V_0=4-64$. Blue traingle stands for DWP with first-level ES from Konwent's analytical results with $V_0=25$ and $A=0.2$.

We now turn our attention to the recently proposed Dong potential [20], given by Eqs. (14) and (15). We obtain the eigen-energy for the Schrödinger equation involving the Dong potential using the filter

method [30]. Using Eq. (16), the threshold condition between DWP with and without ES for first type of Dong potential reads

$$k_{th,ES} = 1.2464a^2 + 5.9717a + 0.044 . \quad (21)$$

Combining with Eq. (16) for critical condition for the existence of DWP, it enables us to define boundary lines for SWP, DWP without ES and DWP with ES for the first type of Dong potential, as shown in **Figure 8(A)**. The validity of our approach is demonstrated by comparing our results in **Figure 8(A)** with those obtained using energy difference method [22]. The structure parameters produce DWP with (without) ES are shown as black (blue) traingles, which align with our prediction. We also compare our prediction with energy function pattern. Here, the presence (absence) of ES is confirmed by the symmetric-antisymmetric pair pattern in the eigenfunction as well as the exponential (linear) dependence of the energy difference on k for $a = 2$ and $k = 20(5)$, reported in Abdurrouf [22].

Using Eq. (16), the threshold condition between DWP with and without ES for second type of Dong potential reads

$$k_{th,ES} = 10.314c + 1.8063 . \quad (22)$$

The results are depicted in **Figure 8(B)**. Numerical data for DWPs with (without) ES, obtained using the filter method [22] and confluent Heun function [20], classified using energy difference method [22], are presented as black (blue) triangles. The figure illustrates the excellent agreement between our predictions and the existing data. In absence of analytical formulae for critical condition between SWP and DWP, we obtain that for $c = 0.1-1$ the DWP exist for $k > 0.0001$.

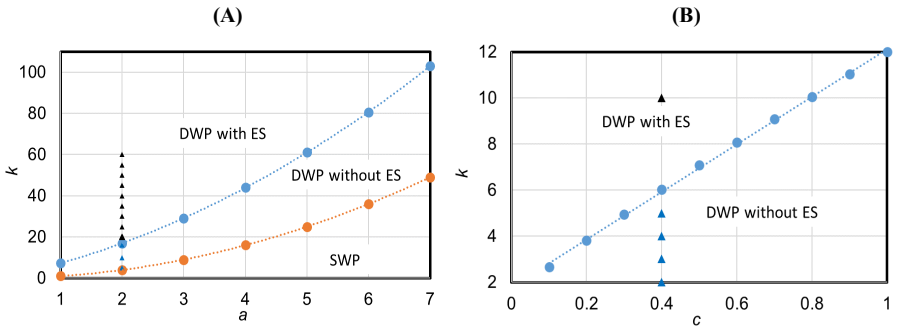

Figure 8 The 3 regimes for the Dong potential (**12**) with with $a = 1-7$ (left panel) and the 2 regimes of the Dong potential (**13**) with with $c = 0.1-1$. The triangles represents the numerical data classified using energy difference methods [22], indicating DWP with ES (black) and without ES (blue).

To summerize, we have derived the critical condition for existence of DWP, first- and some higher level ES in Razavy and Dong classes DWPs. The critical condition are expressed as a function of 2 structure parameters, those are ξ and m for RP potential with $\alpha = 1$, η and M for DSHG potential with $2\beta^2 = 1$, V_0 and A for Konwent potential with $a = 2$, a and k for first type of Dong potential, and c and k for second type of Dong potential.

Conclusions

This study has determined the critical conditions for the emergence of DWPs, as well as first and higher-order ESs, within the Razavy and Dong potential classes. These conditions are expressed as functions of 2 structural parameters. We introduce distinct classifications: SWP, DWP without ES, DWP with first-level ES, DWP with second-level ES and DWP with third-level ES. Our results align well with those obtained using eigenfunction and energy difference methods, as well as the set numerical data obtained

using BAM, AIM and filter method. These findings pave the way for future research in various directions, including (i) extending the critical condition approach to a broader spectrum of potentials and parameter regimes, and (ii) developing strategies for precise control of ES and energy separation within DWP systems.

Acknowledgements

This work was financially supported by Faculty of Mathematics and Natural Sciences Brawijaya University in Indonesia, through "Research of DPP/SPP year 2024" with the contract number: 2612.56/UN01.F09/PN/2024.

References

[1] A Kumar and P Kumar. How the two-center three-electron hemibond affect the inversion barrier of NH_3 in *X*-NH_3 complex (*X* = F, Cl and Br). *Journal of Chemical Sciences* 2024; **136**, 48.

[2] S Halder, S Samaddar, K Purkait, CR Mandal and M Purkait. Two-center interference effects for single electron capture in fast ionmolecule collisions. *Indian Journal of Physics* 2020; **94**, 151-159.

[3] F Correa and O Quintana. Integrable extensions of two-center Coulomb systems. *Physical Review D* 2024; **109(8)**, 085011.

[4] KC Chen. On action-minimizing solutions of the two-center problem. *Acta Mathematica Scientia* 2022; **42(6)**, 2450-2458.

[5] V Jelic and F Marsiglio. The double-well potential in quantum mechanics: A simple, numerically exact formulation. *European Journal of Physics* 2012; **33(6)**, 1651.

[6] M Razavy. An exactly soluble Schrödinger equation with a bistable potential. *American Journal of Physics* 1980; **48**, 285-288.

[7] H Konwent. One-dimensional Schrödinger equation with a new type double-well potential. *Physics Letters A* 1986; **118(9)**, 467-470.

[8] S Habib, A Khare and A Saxena. Statistical mechanics of double sinh-Gordon kinks. *Physica D* 1998; **123(1-4)**, 341-356.

[9] M Gambhir, B Vidhani, S Devi and V Prasad. Impact of asymmetry of Razavy-type coupled well system and static electric field on the time-dynamical studies of entanglement. *The European Physical Journal Plus* 2023; **138**, 57.

[10] A Turkoglu, H Dakhlaoui, ME Mora-Ramos and F Ungan. Optical properties of a quantum well with Razavy confinement potential: Role of applied external fields. *Physica E: Low-Dimensional Systems and Nanostructures* 2021; **134**, 114919.

[11] H Dakhlaoui, JA Gil-Corrales, AL Morales, E Kasapoglu, A Radu, RI Restrepo, V Tulupenko, JA Vinasco, ME Mora-Ramos and CA Duque. Theoretical study of electronic and optical properties in doped quantum structures with Razavy confning potential: Effects of external fields. *Journal of Computational Electronics* 2022; **21**, 378-395.

[12] RJ Hussin and IB Karomi. Ultrashort cavity length effects on the performance of GaInP multiple-quantum-well laser diode. *Results in Optics* 2023; **12**, 100452.

[13] MS Al-Ghamdi, NM Almalky, R Sait, SJ Gillgrass and B Karomi. Effect of barrier layer width on the optical and spectral properties of InAsP/AlGaInP quantum dot lasers. *Optical Materials* 2023; **145**, 114475.

[14] EB Al, E Kasapoglu, S Sakiroglu, H Sari and I Sökmen. Influence of position dependent effective mass on impurity binding energy and absorption in quantum wells with the Konwent potential. *Materials Science in Semiconductor Processing* 2021; **135**, 106076.

[15] M Sayrac, JC Martínez-Orozco, ME Mora-Ramos and F Ungan. The nonlinear optical rectification, second and third harmonic generation coefficients of Konwent potential quantum wells. *The European Physical Journal Plus* 2022; **137**, 1033.

[16] KA Rodríguez-Magdaleno, FM Nava-Maldonado, E Kasapoglu, ME Mora-Ramos, F Ungan and JC Martínez-Orozco. Nonlinear absorption coefficient and relative refractive index change for Konwent potential quantum well as a function of intense laser field effect. *Physica E: Low-Dimensional Systems and Nanostructures* 2023; **148**, 115618.

[17] H Dakhlaoui, W Belhadj, MO Musa and F Ungan. Electronic states and optical

characteristics of GaAs spherical quantum dot based on Konwent-like confining potential: Role of the hydrogenic impurity and structure parameters. *Optik* 2023; **277**, 170684.

[18] H Dakhlaoui, W Belhadj, F Ungan and NS Al-Shameri. Linear and nonlinear optical properties in GaAs quantum well based on Konwent-like potential: Effects of impurities and structural parameters. *Physica E: Low-Dimensional Systems and Nanostructures* 2023; **152**, 115760.

[19] EB Al, E Kasapoglu, H Sari and I Sökmen. Optical properties of spherical quantum dot in the presence of donor impurity under the magnetic field. *Physica B: Condensed Matter* 2021; **613**, 41287.

[20] Q Dong, GH Sun, J Jing and SH Dong. New findings for two new type sine hyperbolic potentials. *Physics Letters A* 2019; **383(2-3)**, 270-275.

[21] AS Durmuslar, CA Billur, A Turkoglu and F Ungan. Optical properties of a GaAs quantum well with new type of hyperbolic confinement potential: Effect of structure parameters and intense laser field. *Optics Communications* 2021; **499**, 127266.

[22] Abdurrouf, G Saroja and M Nurhuda. Estimation of energy separation in tunelling states in symmetric hyperbolicus double-well potential problem using filter method. *Trends in Sciences* 2024; **21(3)**, 7355.

[23] MA Reyes, E Condori-Pozo and C Villasenor-Mora. On the analytical solutions of the quasi-exactly solvable Razavy type potential V(x) = Vo (sinh**4 (x)-k sinh**2 (x)). *arXiv* 2018; **1806**, 03388.

[24] WC Poel. 2011, Energieaufspaltung im Razavy-Potenzial (*in German*). Bachelor's Thesis. Institut für Theoretische Physik, Munster, Germany.

[25] A Fulst. 2011, Analytische und numerische Untersuchungen quasi-exakt lösbarer Potentiale (*in German*). Bachelor's Thesis. Institut für Theoretische Physik, Munster, Germany.

[26] Q Dong, FA Serrano, GH Sun, J Jing and SH Dong. Semi-exact solutions of the Razavy potential. *Advances High Energy Physics* 2018; **2018**, 9105825.

[27] M Baradaran and H Panahi. Exact solutions of a class of double-well potentials: Algebraic bethe ansatz. *Advances in High Energy Physics* 2017; **2017**, 8429863.

[28] AJ Sous. Eigenenergies for the Razavy potential using the asymptotic iteration method. *Modern Physics Letters A* 2007; **22**, 1677-1684.

[29] Q Dong, SS Dong, E Hernández-Márquez, R Silva-Ortigoza, GH Sun and SH Dong. Semi-exact solutions of Konwent potential. *Communications in Theoretical Physics* 2019; **71(2)**, 231.

[30] M Nurhuda and A Rouf. Filter method without boundary-value condition for simultaneous calculation of eigenfunction and eigenvalue of a stationary Schrödinger equation on a grid. *Physical Review E* 2017; **96**, 033302.

[31] Abdurrouf, M Nurhuda and Wiyono. Modelling one-dimensional crystal by using harmonic oscillator potential. *IOP Conference Series: Materials Science and Engineering* 2019; **546**, 052001.

[32] Abdurrouf, MA Pamungkas, W Wiyono and M Nurhuda. Implementation of filter method to solve the Kronig-Penney model. *AIP Conference Proceedings* 2020; **2234(1)**, 040001.

[33] Abdurrouf, MA Pamungkas and M Nurhuda. The energy spectrum of imperfect Kronig-Penney model. *International Journal of Innovative Technology and Exploring Engineering* 2020; **9(3S)**, 205-208.

[34] Abdurrouf, MA Pamungkas and M Nurhuda. Numerical solution of the Schrödinger equation with periodic coulomb potential. *Journal of Physics: Conference Series* 2021; **1825**, 012105.

[35] MK El-Daou, TH AlZanki and NS Al-Mutawa. Quasi-exactly solvable differential models: A canonical polynomials approach. *American Journal of Computational Mathematics* 2019; **9(2)**, 92740.

[36] A Khare and BP Mandal. Anti-isospectral transformations, orthogonal polynomials, and quasi-exactly solvable problems. *Journal of Mathematical Physics* 1990; **39**, 3476-3486.

[37] A Garg. Tunnel splittings for one-dimensional potential wells revisited. *American Journal of Physics* 2000; **68**, 430-437.

[38] AE Sitnitsky. Analytic calculation of ground state splitting in symmetric double well potential. *Computational and Theoretical Chemistry* 2018; **1138**, 15-22.

[39] CM Porto and NH Morgon. Analytical approach for the tunneling process in double well potentials using IRC calculations. *Computational and Theoretical Chemistry* 2020; **1187**, 112917.